

# Conductivity and magnetoresistance of a periodic composite by network discretization

K. D. Fisher and D. Stroud

*Department of Physics, The Ohio State University, Columbus, Ohio 43210*

(Received 16 June 1997)

We describe a simple approach for calculating the effective conductivity, dielectric constant, and magnetoresistance of periodic composites, by reducing the composite to an effective impedance network. The method is used to calculate the effective conductance of periodic two-dimensional binary composites on a square lattice, in good agreement with previous calculations using other methods. We use the same approach to calculate the magnetoresistivity of a periodic composite of parallel perfectly conducting cylinders arranged on a square lattice in a magnetic field perpendicular to the cylinders. We find a striking anisotropy, depending on the angle between the magnetic field and an axis of the square lattice. The anisotropy is explained by means of a percolation argument. [S0163-1829(97)04546-3]

## I. INTRODUCTION

The electrical and magnetic properties of periodic composites have recently been of much theoretical interest.<sup>1-10</sup> In part, this interest has arisen because periodicity makes these properties less difficult to calculate. In addition, advances in microfabrication technology have made it possible to design periodic composites almost to order, especially in two dimensions (2D), even on a submicron scale.<sup>11</sup> While the properties of periodic composites on this scale may often be strongly influenced by quantum effects (such as Josephson tunneling between superconducting grains<sup>12-14</sup>), the “classical” behavior of these composites (i.e., those properties which are primarily determined by solutions of Maxwell’s equations in a periodic composite) are still of interest, and may even dominate some experimentally observed behavior.

The basic “classical” problem of interest is simply the following: given a conductor, described by a periodic conductivity  $\sigma(\mathbf{x})$  in  $d$  dimensions (where  $d$  is typically 2 or 3), what is the effective conductivity  $\sigma_e$  of the composite as a whole? In a binary composite,  $\sigma(\mathbf{x})$  will usually take on either of two values, say  $\sigma_1$  or  $\sigma_2$ , depending on whether the spatial point  $\mathbf{x}$  lies within material 1 or 2. At sufficiently low frequencies, this problem can be treated by solving Maxwell’s equations in the appropriate quasistatic limit, i.e., by finding the appropriate electrostatic potential; this is the regime we consider here. It is worth noting that a range of other, seemingly different, problems are described by formally identical equations. Among these are finding the effective dielectric function of an inhomogeneous dielectric and the effective magnetic permeability of an inhomogeneous paramagnetic material.

A wide range of theoretical methods have been applied to this problem in the literature. For example, Fourier expansion techniques have achieved excellent results<sup>2-4,6,7</sup> in a range of periodic composites. They may be applied when the constituents are isotropic conductors or dielectrics, and may even be extended to anisotropic constituents. Other approaches include series expansions of the electric potential,<sup>5</sup> Green’s-function methods,<sup>8</sup> and techniques which use the analyticity of the composite effective dielectric function  $\epsilon$ ,

viewed as a function of the ratio  $\epsilon_1/\epsilon_2$  of the constituent dielectric functions.<sup>9</sup>

In this paper, we describe a simple alternative scheme for treating such composites, which focuses attention on a single unit cell in real space. The scheme, a natural outgrowth of the method described in Ref. 15, is basically to represent a unit cell of the periodic conductor as a ( $d$ -dimensional) square or cubic impedance network. The network is easy to construct, and the calculations are readily carried out for a wide range of geometries. Indeed, with sufficient computing power and memory, it will allow results as accurate as desired. Finally, the same approach is readily extended to complex impedances, as well as to periodic composites whose constituents are anisotropic.

To illustrate this approach, we apply it, first, to an isotropic binary periodic composite on a square lattice in 2D, but with the inclusions chosen to be of several different shapes (Fig. 1). The effective conductance, not surprisingly, shows a strong shape dependence, and also exhibits a percolation threshold which depends on the inclusion shape. The calculated results agree fairly well with a simple analytical approach (the so-called Maxwell-Garnett approximation). When comparison is possible, they are also in excellent agreement with more sophisticated Green’s function or Fourier approaches.<sup>1,4,8</sup> For each shape, a kind of percolation transition is achieved by increasing the linear dimensions of the inclusions isotropically until they form a continuous path through the sample. The effective conductivity near this percolation transition does not, however, appear to show a non-integer power-law dependence on  $p - p_c$ , the deviation of inclusion areal fraction  $p$  from the percolation fraction  $p_c$ . Such a nonintegral power-law dependence is typical of percolation transitions in random composites,<sup>16</sup> and is presumably absent here because the composite is periodic.

As a second application, we consider the magnetoresistance of a simple model for a periodic composite of superconducting inclusions in a normal metal host. The inclusions are modeled as identical, perfectly conducting, parallel cylinders arranged on a square lattice. The magnetic field is applied normal to the cylinder axis, but at different angles  $\theta$  to the symmetry axis of the square lattice. A slice of this composite normal to the cylinder axis could be interpreted as

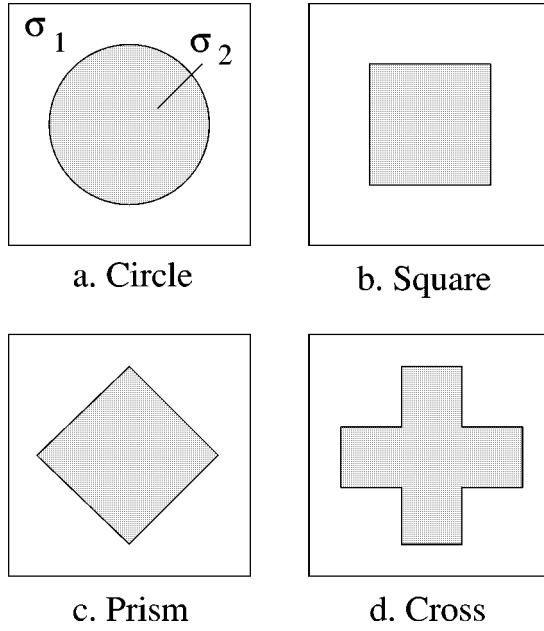


FIG. 1. Inclusion shapes for each 2D composite studied here. Materials inside and outside the inclusion have conductivities  $\sigma_2$  and  $\sigma_1$ , with  $\sigma_2/\sigma_1 > 1$ . Each large square represents one unit cell of a square array. In each case, the areal fraction of material 2 is increased by uniformly increasing the linear dimensions of the inclusions.

a two-dimensional normal-superconducting (NS) array with a magnetic field parallel to the film. While the model omits quantum effects such as Josephson coupling between different superconducting inclusions, it does include the “classical” effects which are known to be experimentally important in NS composites.<sup>17</sup> We find that both the transverse and the longitudinal magnetoresistance of this array, calculated using our single-cell numerical method, depend strongly on the angle  $\theta$ . The anisotropy can be explained using a simple percolation argument.

We turn now to the body of the paper. In Sec. II, we describe the approach, for both isotropic periodic composites, and NS composites in the presence of magnetic-field-produced anisotropy. Our numerical results are given in Secs. III and IV, followed by a short discussion in Sec. V.

## II. METHOD

### A. Scalar effective conductivity

To describe the method, we imagine we are dealing with a periodic composite medium, usually in two or three dimensions— $d=2$  or 3. That is, the electric field  $\mathbf{E}(\mathbf{r})$  and current density  $\mathbf{J}(\mathbf{r})$  in the composite are related by the equation

$$\mathbf{J}(\mathbf{r}) = \sigma(\mathbf{r})\mathbf{E}(\mathbf{r}), \quad (1)$$

where  $\sigma(\mathbf{r})$ , the position-dependent conductivity, is a periodic function of position. For convenience, we initially assume that  $\sigma(\mathbf{r})$  is a *scalar*, though in general it may be a  $3 \times 3$  matrix.

The differential equations of electrostatics describing this composite are  $\nabla \cdot \mathbf{J} = 0$  and  $\nabla \times \mathbf{E} = 0$ . The latter equation

implies that the electric field can be written as  $\mathbf{E} = -\nabla\Phi$ , where  $\Phi$  is a scalar potential. Combining these relations gives

$$\nabla \cdot (\sigma(\mathbf{r})\nabla\Phi) = 0. \quad (2)$$

Nothing thus far implies that the composite is necessarily periodic.

A natural way to solve a partial differential equation is by discretizing it. Thus, a derivative such as  $\partial\Phi/\partial x$  is represented as a finite difference:  $\partial\Phi/\partial x = [\Phi(x+\Delta, y, z) - \Phi(x, y, z)]/\Delta$ . Here  $\Delta$  is the grid dimension, and in the limit of small  $\Delta$ , such discretization will become exact. When this procedure is applied to the partial differential equation for  $\Phi$ , the equation becomes equivalent to Kirchhoff's Laws for a square or cubic conductance network with grid size  $\Delta$ . The equations may be written

$$\sum_j g_{ij}(V_i - V_j) = 0, \quad (3)$$

where  $V_i$  is the voltage on the  $i$ th node and  $g_{ij}$  is the conductance between nearest neighbor nodes  $i$  and  $j$ . A discretization of this form has frequently been discussed (see, e.g., Ref. 16).

Now consider a periodic composite. Then the conductances of the network will repeat themselves periodically in space, and it should be necessary to consider only one unit cell of the composite. In order to accomplish this, we write the potential as the sum of one part arising from a uniform applied electric field  $\mathbf{E}_0$ , and another due to deviations from uniformity. Thus

$$V_i = -\mathbf{E}_0 \cdot \mathbf{r}_i + V'_i, \quad (4)$$

where  $\mathbf{r}_i$  is the position of the  $i$ th node,  $-\mathbf{E}_0 \cdot \mathbf{r}_i$  is the potential due to the uniform field, and  $V'_i$  is the remainder of the potential. If the composite is, indeed, homogeneous (so that all the  $g_{ij}$ 's are equal), then the uniform electric field would be an allowed solution.

Substituting Eq. (4) back into the Kirchhoff equations, we get a set of inhomogeneous equations for the  $V'_i$ 's:

$$\sum_j g_{ij}(V'_i - V'_j) = \Gamma_i, \quad (5)$$

where

$$\Gamma_i = \sum_j g_{ij}\mathbf{E}_0 \cdot (\mathbf{r}_i - \mathbf{r}_j). \quad (6)$$

Given the particular distribution of  $g_{ij}$ 's, and given the applied field  $\mathbf{E}_0$ , the  $\Gamma_i$ 's are known. The potentials  $V'_i$ , and hence all the local fields and currents, can then be found simply by inverting this set of inhomogeneous linear equations.

To specialize to a periodic composite, we need only specify that the potentials  $V'_i$  repeat periodically. (Note that the *total* potential does *not* repeat periodically, because that part of the potential which specifies the uniform applied field increases linearly with  $\mathbf{r}$ .) Thus, we need only consider a single unit cell of this composite, represent the inhomogeneous conductivity of that cell by an appropriate conduc-

tance network, and apply periodic boundary conditions (in two or three dimensions, as appropriate). We can use as dense a network as we like to treat the single unit cell, thus allowing, in principle, considerable accuracy in the results.

The linear equations can readily be solved numerically by a variety of methods. For example, we have found that a straightforward iterative method converges well for several cases we have considered.<sup>16</sup> Namely, we can rewrite the network equations in the form

$$\left( \sum_j g_{ij} \right) V'_i = \left( \Gamma_i + \sum_j g_{ij} V'_j \right). \quad (7)$$

Then we guess a trial form for the  $V'_j$ , called  $V'_j{}^0$ . The  $(n+1)$ th iteration is obtained from the  $n$ th using the equations

$$V'_i{}^{n+1} = \left( \Gamma_i + \sum_j g_{ij} V'_j{}^n \right) / \left( \sum_j g_{ij} \right), \quad (8)$$

and the equations are iterated to convergence. Once the local potentials and currents are thus determined, the effective conductance is easily calculated via

$$g_{\alpha\alpha}^e = \frac{\langle I_\alpha \rangle}{\langle -(\Delta V)_\alpha \rangle}, \quad (9)$$

where  $I_\alpha$  and  $(\Delta V)_\alpha$  denote the current and voltage drop across a single bond in the  $\alpha$  direction ( $\alpha = x, y, z$ ), and the averages are taken over a unit cell of the network. The same method also permits one to obtain the electric-field distribution, if desired.<sup>15,16</sup>

### B. Magnetoresistance in periodic composites

This approach is not limited to calculating effective conductivity in isotropic composites. It can also be applied to intrinsically *anisotropic* problems, such as the magnetoresistance in periodic composites. In the presence of an external magnetic field, the conductivity  $\hat{\sigma}(\mathbf{r})$  is no longer a scalar, or even a diagonal tensor. To describe a composite in the presence of a magnetic field, therefore, we first separate the conductivity tensor into diagonal and off-diagonal parts,

$$\hat{\sigma}(\mathbf{r}, \mathbf{H}) = \hat{\sigma}^d(\mathbf{r}, \mathbf{H}) + \hat{\sigma}^a(\mathbf{r}, \mathbf{H}), \quad (10)$$

where, in general, both  $\hat{\sigma}^d$  and  $\hat{\sigma}^a$  will be position dependent. In the present work, we will consider only a special case satisfying the following assumptions:  $\sigma_{ij}^a = -\sigma_{ji}^a$  and  $\hat{\sigma}^a \neq \hat{\sigma}^a(\mathbf{r})$ . The first assumption will be valid for many materials in a magnetic field  $\mathbf{H}$ . The second assumption is obviously valid only for materials in which the Hall conductivity is position independent. While this assumption fails for many composites, we argue below that it can be considered valid for a composite of normal free-electron metal ( $N$ ) and perfect conductor ( $S$ ). For simplicity, we will consider only a two-component composite, though the approach can be generalized to any number of components.

We choose the external magnetic field to lie along the  $z$  axis (see Fig. 2). Then the conductivity tensor in the normal (free-electron) material is given by

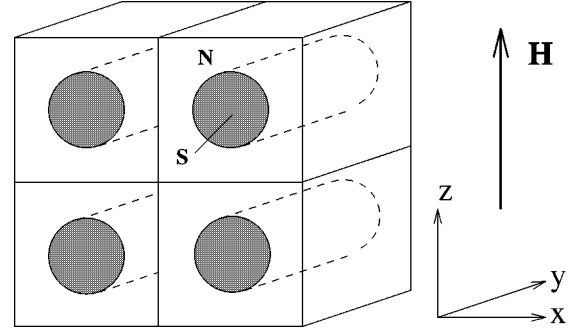


FIG. 2. Model composite geometry used in magnetoresistance calculations. The  $S$  inclusions are taken as infinite along the  $y$  direction. In one calculation,  $\mathbf{H}$  is taken along one of the axes of the square lattice, as shown; in another,  $\mathbf{H}$  is rotated by  $45^\circ$  in the plane of the lattice.

$$\begin{aligned} \hat{\sigma}_N &= \hat{\sigma}_N^d + \hat{\sigma}^a(H) = \sigma_{N_0} \begin{pmatrix} \frac{1}{1+H^2} & 0 & 0 \\ 0 & \frac{1}{1+H^2} & 0 \\ 0 & 0 & 1 \end{pmatrix} \\ &+ \sigma_{N_0} \begin{pmatrix} 0 & \frac{H}{1+H^2} & 0 \\ \frac{-H}{1+H^2} & 0 & 0 \\ 0 & 0 & 0 \end{pmatrix} \\ &= \sigma_{N_0} \begin{pmatrix} \frac{1}{1+H^2} & \frac{H}{1+H^2} & 0 \\ \frac{-H}{1+H^2} & \frac{1}{1+H^2} & 0 \\ 0 & 0 & 1 \end{pmatrix}. \end{aligned}$$

Here  $H = \omega_c \tau$  is the dimensionless magnetic-field strength,  $\omega_c = eB/(mc)$  being the cyclotron frequency (where  $B$  is the magnetic induction,  $e$  is the electronic charge,  $m$  is the electron mass, and  $c$  is the speed of light), and  $\tau$  is a characteristic relaxation time.

In the perfect conductor, we write the conductivity tensor as

$$\hat{\sigma}_S = \hat{\sigma}_S^d + \hat{\sigma}^a(H) = \sigma_{S_0} \hat{I} + \hat{\sigma}^a(H), \quad (11)$$

where  $\hat{I}$  is the  $3 \times 3$  unit matrix, and we later take the limit  $\sigma_{S_0} \rightarrow \infty$ . With this assumption, the antisymmetric part of the total conductivity tensor is position independent as required. While the magnitude of the antisymmetric part in the  $S$  component has no physical significance, it becomes irrelevant in the limit of large  $\sigma_{S_0}$ . Thus, our model is reasonable for treating the ‘‘classical’’ properties of a composite of normal metal and perfect conductor,<sup>17</sup> i.e., those which are determined by the solution of Maxwell’s equations in an inhomogeneous medium.

geneous conductor. It would need to be modified if quantum phenomena such as Josephson coupling are important.

With these assumptions, the off-diagonal terms of Eq. (2) cancel out. The remaining diagonal problem can be discretized on a square or cubic lattice in the form of Eq. (3). The potential at each site of the lattice is now determined entirely by the *diagonal* elements of the conductivity tensor. The corresponding diagonal elements  $\sigma_{\alpha\alpha}^e(H)$  of the effective conductivity tensor are then obtained by considering an electric field  $\langle E_\alpha \rangle$  applied in the  $\alpha$ th direction and finding the resulting space-averaged current density  $\langle J_\alpha \rangle$ :

$$\sigma_{\alpha\alpha}^e(H) = \frac{\langle J_\alpha \rangle}{\langle E_\alpha \rangle}. \quad (12)$$

The off-diagonal elements are, of course, just the elements of  $\hat{\sigma}^a(\mathbf{H})$ .

If the geometry happens to possess translational invariance along one axis, the problem can be further reduced to only two dimensions. As further discussed in Sec. IV below, we choose this direction to be perpendicular to the  $\mathbf{H}$  field and denote it as the  $y$  axis. The problem we consider is then equivalent to a periodic array of parallel cylinders, with the magnetic field applied in a direction perpendicular to the cylinders. The geometry is shown in Fig. 2. The results of calculations in this geometry should be applicable to the observed transport properties of a thin slice of such a composite taken perpendicular to the cylinder axis, i.e., to a 2D normal-superconducting array with magnetic field parallel to the plane of the array, in the ‘‘classical’’ regime.

In the  $y$  direction, the  $N$  and  $S$  components of the composite are connected in parallel. Thus, in the limit of large  $\sigma_{S_0}$ ,  $\sigma_{yy}^e \approx p\sigma_{S_0}$ , where  $p$  is the areal fraction of high-conductivity inclusions; this result is valid because the contribution from  $\hat{\sigma}_N$  is negligible in this direction. The effective conductivity tensor can then be written as

$$\hat{\sigma}^e \approx \begin{pmatrix} \sigma_{xx}^e & \sigma_{xy} & 0 \\ -\sigma_{xy} & p\sigma_{S_0} & 0 \\ 0 & 0 & \sigma_{zz}^e \end{pmatrix},$$

where  $\sigma_{xy} = \sigma_{N_0}H/(1+H^2)$ . Inverting this expression, and taking the limit  $\sigma_{S_0} \rightarrow \infty$ , we find a very simple form for the resistivity tensor:

$$\hat{\rho}^e = \begin{pmatrix} \frac{1}{\sigma_{xx}^e} & 0 & 0 \\ 0 & 0 & 0 \\ 0 & 0 & \frac{1}{\sigma_{zz}^e} \end{pmatrix}.$$

[In the special case  $p=0$ , of course, the effective resistivity tensor is entirely different from this form—it is simply the inverse of the normal conductivity tensor ( $\hat{\rho}^e = (\hat{\sigma}_N)^{-1}$ ).] Thus, once the diagonal elements of  $\hat{\sigma}^e(\mathbf{H})$  are calculated, the effective transverse and longitudinal magnetoresistances of the composite are simply obtained from the definition

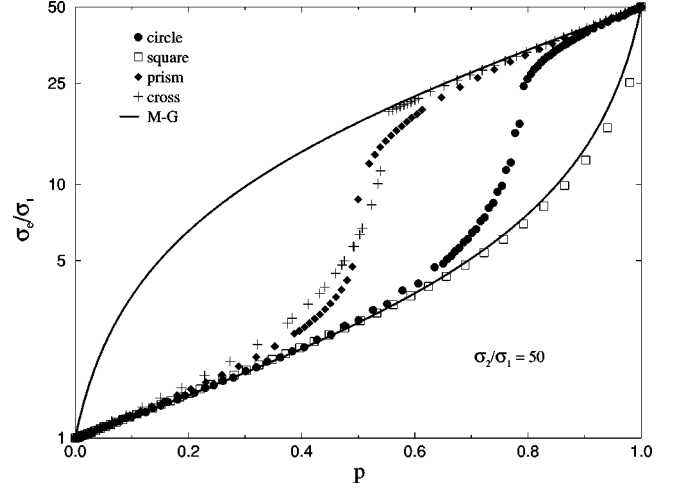


FIG. 3.  $\sigma_e/\sigma_1$  plotted as a function of inclusion areal fraction  $p$  for four inclusion shapes at contrast  $\sigma_2/\sigma_1=50$ .  $p_c = 0.50, 0.56, 0.79$ , and  $1.0$  for prisms, crosses, circles, and squares. Maxwell-Garnett (MG) results are shown for comparison; in the upper MG curve,  $\sigma_2$  and  $\sigma_1$  have been exchanged.

$$\Delta\rho_{\alpha\alpha}^e = \frac{\rho_{\alpha\alpha}^e(H) - \rho_{\alpha\alpha}^e(0)}{\rho_{\alpha\alpha}^e(0)} = \frac{\sigma_{\alpha\alpha}^e(0)}{\sigma_{\alpha\alpha}^e(H)} - 1. \quad (13)$$

In Sec. IV, we present the results of several calculations using this model.

### III. ISOTROPIC CONDUCTIVITY

To illustrate this approach, we have considered a set of periodic two-dimensional composites with isotropic conductivities. Specifically, we have assumed a square unit cell with inclusions of four different shapes (Fig. 1): circular, square, prismatic, and cross shaped. Our crosses have arms of equal lengths and widths; see Fig. 1(d). Except for the square, each shape leads to a network of inclusions which percolates (i.e., forms an infinite connected path) for some areal fraction  $p = p_c < 1$ . ( $p_c = 0.50, 0.56, 0.79$  for the prismatic, cross shaped, and circular inclusions, respectively.) For inclusions of each shape, we increase  $p$  by uniformly increasing the linear dimensions of the inclusions. For  $p > p_c$ , when the inclusions start to overlap, we interpret every point in the plane which is covered by at least one inclusion to have conductivity  $\sigma_2$ .

Figure 3 shows the ratio of  $\sigma_e$  to the host conductivity  $\sigma_1$  for this network as a function of areal inclusion fraction  $p$  for a conductivity contrast  $r = \sigma_2/\sigma_1 = 50$ . For comparison, we also show the predictions of the 2D Maxwell-Garnett (MG) approximation<sup>18</sup>

$$\sigma_e = \sigma_1 \frac{1+pt}{1-pt}, \quad (14)$$

where  $t = (\sigma_2 - \sigma_1)/(\sigma_2 + \sigma_1)$ . The lower MG curve displays this approximation, and the upper curve is the MG approximation with the roles of  $\sigma_1$  and  $\sigma_2$  reversed. The effect of percolation can easily be seen. The array with square inclusions agrees best with the MG prediction, even though it is typically derived in 2D for random, circular inclusions. This behavior is, however, easily understood: of all

TABLE I. Scaled effective dielectric constant  $\epsilon_e/\epsilon_1$  tabulated as a function of contrast  $\epsilon_2/\epsilon_1$  for a 2D periodic composite with prismatic inclusions, as calculated in Milton, McPhedran, and McKenzie (Ref. 1), Bergman and Dunn (Ref. 4), and in the present work. Our calculations are performed on a  $50 \times 50$  network, except where otherwise noted. (Exactly equivalent results would be obtained from a calculation of the effective conductivities.)

| $p$                             | $\epsilon_2/\epsilon_1=2$ | 5       | 10                | 20                | 50              | 100             |
|---------------------------------|---------------------------|---------|-------------------|-------------------|-----------------|-----------------|
| Milton, McPhedran, and McKenzie |                           |         |                   |                   |                 |                 |
| 0.1                             | 1.0696                    | 1.1490  | 1.1904            | 1.2162            | 1.2339          | 1.2402          |
| 0.2                             | 1.1445                    | 1.3239  | 1.4251            | 1.4910            | 1.5377          | 1.5548          |
| 0.3                             | 1.2255                    | 1.5359  | 1.7299            | 1.8654            | 1.9662          | 2.0039          |
| 0.4                             | 1.3141                    | 1.8079  | 2.1683            | 2.4518            | 2.6830          | 2.775           |
| 0.5                             | 1.4142                    | 2.236   | 3.162             | 4.47              | 7.07            | 10              |
| Bergman and Dunn                |                           |         |                   |                   |                 |                 |
| 0.1                             | 1.0697                    | 1.1505  | 1.1969            | $1.235 \pm 0.002$ | $1.29 \pm 0.01$ | $1.34 \pm 0.05$ |
| 0.2                             | 1.1447                    | 1.3284  | $1.441 \pm 0.001$ | $1.528 \pm 0.002$ | $1.63 \pm 0.04$ | $1.7 \pm 0.1$   |
| 0.3                             | 1.2254                    | 1.5385  | $1.748 \pm 0.005$ | $1.93 \pm 0.03$   | $2.2 \pm 0.1$   | $2.4 \pm 0.3$   |
| 0.4                             | 1.3144                    | 1.8151  | $2.199 \pm 0.006$ | $2.54 \pm 0.04$   | $3.0 \pm 0.2$   | $3.3 \pm 0.5$   |
| 0.5                             | 1.4142                    | 2.2404  | 3.2105            | $4.766 \pm 0.001$ | $8.87 \pm 0.01$ | $15.4 \pm 0.2$  |
| Present work                    |                           |         |                   |                   |                 |                 |
| 0.1                             | 1.06979                   | 1.14986 | 1.19205           | 1.21855           | 1.23685         | 1.24343         |
| 0.2                             | 1.14471                   | 1.32529 | 1.42786           | 1.49525           | 1.54323         | 1.56078         |
| 0.3                             | 1.22581                   | 1.53831 | 1.73546           | 1.87442           | 1.9785          | 2.01774         |
| 0.4                             | 1.31457                   | 1.81278 | 2.18226           | 2.478             | 2.72346         | 2.82219         |
| 0.5                             | 1.41487                   | 2.256   | 3.29471           | 5.06918           | 10.002          | 18.0497         |
| (100×100 array)                 |                           |         |                   |                   |                 |                 |
| 0.5                             | 1.41444                   | 2.4553  | 3.23874           | 4.86857           | 9.25866         | 16.3393         |
| (140×140 array)                 |                           |         |                   |                   |                 |                 |
| 0.5                             | 1.41435                   | 2.24267 | 3.22092           | 4.79795           | 8.9771          | 15.6732         |
| (200×200 array)                 |                           |         |                   |                   |                 |                 |
| 0.5                             | 1.41429                   | 2.24057 | 3.20659           | 4.7372            | 8.72211         | 15.058          |

the shapes considered, only the squares have a percolation threshold  $p_c = 1$ , as predicted by the MG approximation. The other geometries all have  $p_c < 1$ , and among these, the circular case does most closely resemble the MG predictions below  $p_c$ .

Near  $p = 1$ ,  $\sigma_e$  varies approximately linearly with  $p$  in all samples except those with square inclusions. To a good approximation, the slope in this regime is  $d\sigma_e/dp = +2\sigma_2$  for the other three cases. This slope is in excellent agreement with both the effective-medium approximation in 2D, and the MG approximation for poorly conducting inclusions  $\sigma_1$  in a host of conductivity  $\sigma_2$  (upper MG curve), both of which also agree with the exact result in the limit of small  $1-p$ .<sup>9</sup> Cross-shaped samples show the best agreement, since, above  $p_c = 0.56$ , they become square inclusions  $\sigma_1$  embedded in a host of conductivity  $\sigma_2$ . Presumably, this linear dependence would become exact in the limit of large contrast for any  $p > p_c$ , since in that regime, all the current would flow through the high-conductivity material. Square inclusions, of course, do not exhibit this slope because for all  $p < 1$  all the square samples lie below the percolation threshold.

Note that, because of the discreteness of the grid, our approach does not permit a completely arbitrary choice of  $p$ . This discreteness problem is probably worst for the circular inclusions, which can only be approximately realized on a square grid. This effect may account for the slight noisiness

of the data in Fig. 3 (and also in Fig. 5 below). Both of these minor deficiencies can, of course, be mitigated to any desired extent by using a finer grid.

The electrostatic equations which determine effective conductivity are formally identical to those which determine the bulk effective dielectric constant  $\epsilon_e$  in a composite of two different dielectrics. Because of this formal analogy, our results can be compared to some recent calculations of  $\epsilon_e$ , based on other approaches. Table I shows  $\epsilon_e$ , as calculated for a periodic dielectric consisting of prismatic inclusions of dielectric constant  $\epsilon_2$  embedded in a host of dielectric constant  $\epsilon_1$ , using various approaches. The results are tabulated as a function of  $p$  ( $< p_c$ ) and  $\epsilon_2/\epsilon_1$ . The top two panels show the results of Milton *et al.*<sup>1</sup> and of Bergman and Dunn,<sup>4</sup> using analytical approximations. The bottom panel shows our calculations (based mostly on a  $50 \times 50$  network unless otherwise noted). Evidently, our results are in excellent agreement with those of Ref. 4, except close to  $p_c$ , where apparently an extremely fine mesh is required to achieve agreement. We view these results as evidence that our simple numerical approach gives accurate results even in the case of fairly large contrast and large defect concentration. We believe that our results deviate from those of Milton *et al.* precisely at percolation (where the results of Milton *et al.* are exact) simply because of our finite-density grid. In support of this conjecture, we note that our results just at  $p_c$  more closely approach those of Ref. 1 as the grid becomes finer.<sup>19</sup>

While most of our geometries exhibit percolation at an areal fraction  $p_c < 1$ ,  $\sigma_e$  near  $p_c$  does *not* behave as it does for percolation in a *random* composite. In the random case, it is thought that (in the limit  $\sigma_2/\sigma_1 \gg 1$ )  $\sigma_e \approx \sigma_1(p_c - p)^{-s}$  for  $p < p_c$  and  $\sigma_e \approx \sigma_2(p - p_c)^t$  for  $p > p_c$ , with  $s = t \approx 1.30$  in  $d = 2$ .<sup>16,20,21</sup> For the present case of *periodic* percolation, although we have not made a careful study near  $p_c$ , Fig. 3 suggests that the analytical form of  $\sigma_e(p)$  will be quite different, and also that it may depend on the inclusion shape. We speculate that the seeming discontinuous jump in  $\sigma_e/\sigma_1$  near  $p_c$  is just an artifact of our finite grid density.

#### IV. MAGNETORESISTANCE IN A PERIODIC NORMAL/ PERFECT CONDUCTOR COMPOSITE

Next, we consider the magnetoresistance of a periodic composite. Specifically, we study a periodic array of parallel, perfectly conducting cylinders embedded in a normal host, using the model of Sec. II B. The magnetic field and cylinder axes are taken as the  $z$  and  $y$  directions, respectively. Figure 2 shows an example of such a geometry: a square array of right circular cylinders, with  $\mathbf{H}$  perpendicular to the cylinders and parallel to an axis of the square array. We have also considered another geometry, in which  $\mathbf{H}$  is still perpendicular to the cylinders but oriented at a  $45^\circ$  angle to an axis of the square array. These choices allow us to probe the variation of magnetoresistance with field orientation. In actual calculations, we used  $\sigma_{N_0} = 1$  and  $\sigma_{S_0} = 10^8$ . In each geometry, we calculate both the transverse and the longitudinal magnetoresistance, i.e., (taking  $\mathbf{H} \parallel z$ )  $\Delta\rho_{xx}(H) \equiv [\rho_{xx}(H) - \rho(0)]/\rho(0)$  and  $\Delta\rho_{zz}(H) \equiv [\rho_{zz}(H) - \rho(0)]/\rho(0)$ , where  $\rho(0)$  is the zero-field resistivity in the  $xz$  plane.

Figure 4 shows  $\Delta\rho_{xx}(H)$  and  $\Delta\rho_{zz}(H)$  for several values of volume fractions  $p < p_c = 0.79$  of  $S$  inclusions, and two orientations of  $\mathbf{H}$  in the plane perpendicular to the cylinder axis. In both orientations, there is clear evidence of anisotropy between  $\Delta\rho_{xx}(H)$ , which usually increases without bound for a given  $p$ , and  $\Delta\rho_{zz}(H)$ , which always saturates at high fields. The same behavior is exhibited differently in Fig. 5, where we show the magnetoresistances plotted versus  $p$  at several fixed values of  $H$ . For most values of  $p$ , the transverse magnetoresistance varies roughly as  $H^2$ . We have therefore divided  $\Delta\rho_{xx}(p)$  by a factor  $H^2$  in Figs. 5(a) and 5(b). The longitudinal magnetoresistance has not been similarly scaled [Figs. 5(c) and 5(d)].

Both components of magnetoresistance fall to zero at  $p = p_c$ , and do so more or less sharply depending upon the orientation and strength of  $\mathbf{H}$ . This behavior is to be expected, since, once the  $S$  component percolates, the composite as a whole should be perfectly conducting. For orientation  $I$  ( $\mathbf{H}$  parallel to one of the axes of the square lattice), at each field strength shown,  $\Delta\rho_{zz}$  first rises to a maximum at  $p \approx 0.35$  then falls back to zero. This result is reminiscent of an earlier calculation,<sup>17</sup> which found a peak in the *transverse* magnetoresistance in a three-dimensional NS composite with random, spherical  $S$  inclusions. Possibly, the topological differences between the two models account for the fact that, in our model, the peak appears in the longitudinal magnetoresistance. As in Fig. 4, there is a large difference between  $\Delta\rho_{xx}$  and  $\Delta\rho_{zz}$ .

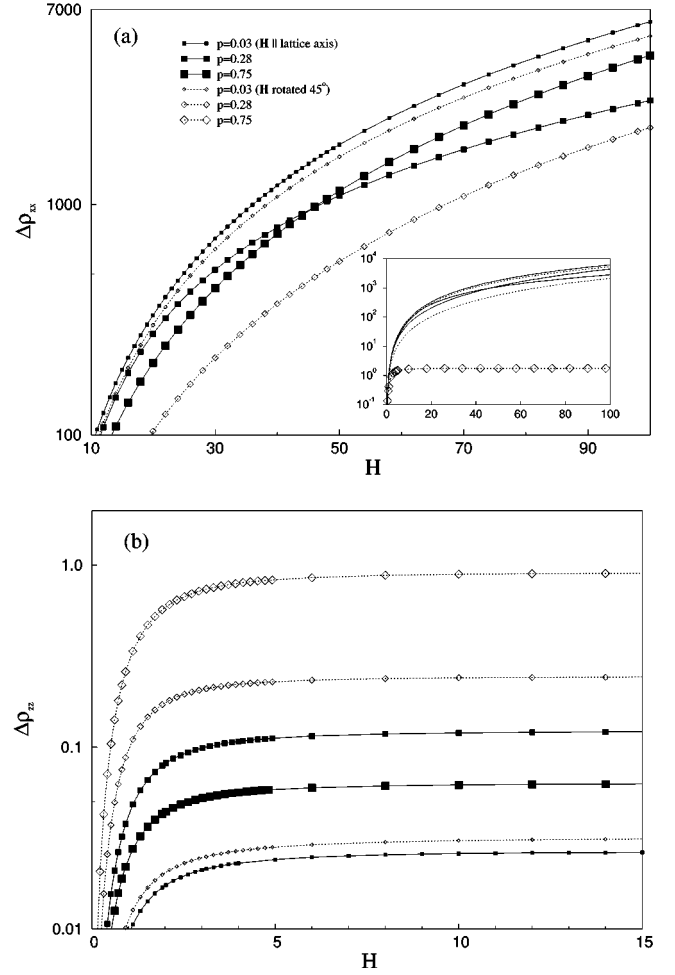


FIG. 4. Anisotropy and field dependence of magnetoresistance in quasi-three-dimensional NS composites. The inclusions are infinitely long, perfectly conducting, right circular cylinders. (a) Transverse magnetoresistance  $\Delta\rho_{xx}$ . Solid squares with solid lines correspond to the field orientation in Fig. 2. Open diamonds with dotted lines correspond to a rotation of the external magnetic field by  $45^\circ$  about the  $y$  axis. The inset compares  $p = 0.75$  for the rotated field geometry to the other cases. (b) Longitudinal magnetoresistance  $\Delta\rho_{zz}$  for same fields and geometries. In all cases (and later figures), line segments simply interpolate between calculated points.

The anisotropy between  $\Delta\rho_{xx}(H, p)$  and  $\Delta\rho_{zz}(H, p)$  is not very surprising, since the conductivity tensor of the normal metal is highly anisotropic. More remarkable is the strong anisotropy as a function of magnetic-field orientation in the  $xz$  plane. We now argue that this anisotropy is due to a percolationlike effect. The argument is most easily presented for  $\Delta\rho_{xx}(H, p)$ , the component of magnetoresistance perpendicular to the magnetic field. In this case, according to Sec. II B, the normal metal can be treated as an anisotropic network, with much higher conductances parallel than perpendicular to  $\mathbf{H}$ . In the perpendicular (i.e., the  $x$ ) direction, therefore,  $\rho_{xx}^e$  will be large *unless* the current can find a path which runs entirely in the  $z$  direction in the normal metal, but in either direction in the perfect conductor. Such a path will be possible only if the areal fraction of superconductor exceeds a certain critical fraction  $p_c^*(\theta)$ , where  $\theta$  is the angle

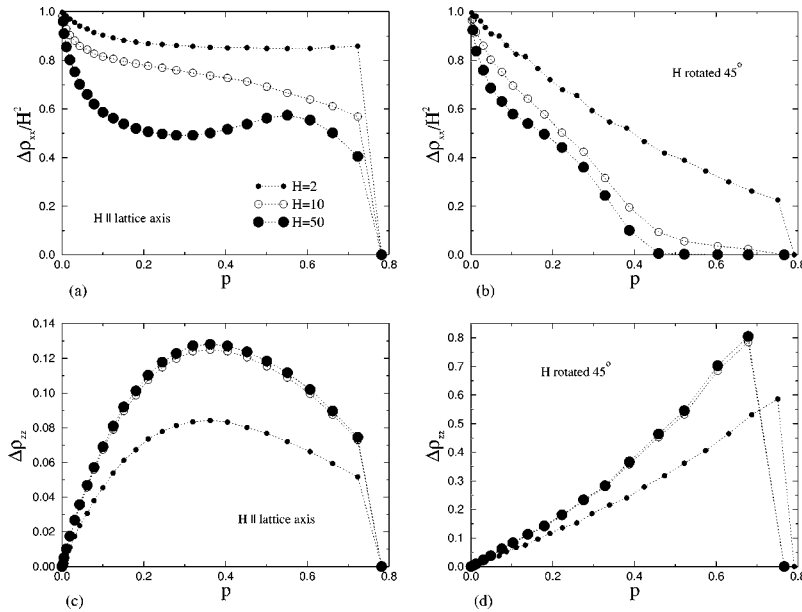


FIG. 5. Magnetoresistance plotted versus inclusion volume fraction  $p$  (for  $p < p_c = 0.79$ ) at three different field strengths and two different field orientations, for cylindrical  $S$  inclusions with circular cross section. (a) Transverse magnetoresistance  $\Delta\rho_{xx}(H,p)/H^2$ , with  $\mathbf{H}$  oriented in the  $xz$  plane parallel to the lattice symmetry axis. (b)  $\Delta\rho_{xx}(H,p)/H^2$  with  $\mathbf{H}$  rotated  $45^\circ$  from the lattice axis, still in the  $xz$  plane. (c) Longitudinal magnetoresistance  $\Delta\rho_{zz}(H,p)$  (not scaled by  $H^2$ ), with  $\mathbf{H}$  parallel to the lattice symmetry axis. (d)  $\Delta\rho_{zz}(H,p)$  with  $\mathbf{H}$  rotated by  $45^\circ$ . In all these figures, the lattice is perpendicular to the  $y$  axis, and  $\mathbf{H} \parallel z$ .

between the magnetic field and one of the axes of the square lattice.

For  $\theta = \pi/4$ , it is readily verified that  $p_c^*(\pi/4) = \pi/8 \approx 0.39$ . Thus, for  $\theta = \pi/4$ , we expect  $\Delta\rho_{xx}$  to drop dramatically at  $p \approx p_c^*(\pi/4)$ , especially at large fields  $H$  where the anisotropy of the normal metal is greatest. For  $\theta = 0$ , on the other hand,  $p_c^*(0) = \pi/4 = 0.79$ , equal to the actual percolation threshold; so no such drop should be observed until the composite as a whole becomes perfectly conducting. Indeed, the numerical results of Figs. 4 and 5 show just such percolation behavior. The values of  $p_c^*$  may, however, be shifted slightly relative to the above predictions, which are accurate only for asymptotically large  $H$  fields.

The actual value of  $p_c^*(\theta)$  can be determined by a simple graphical construction which is illustrated in Fig. 6 for circular cylinders on a square lattice. To find  $p_c^*(\theta)$  at any given  $\theta$ , one constructs a straight line at angle  $\theta$  to one axis of the lattice, as shown.  $p_c^*(\theta)$  is the smallest value of  $p$  such that any such straight line is sure to intersect some of the perfectly conducting cylinders. For most values of  $\theta$ , we expect  $p_c(\theta)$  to be quite small, possibly zero, but for selected  $\theta$ 's such that  $\tan\theta$  is a rational number  $p/q$  with  $p$  and  $q$  small integers,  $p_c^*(\theta)$  will be nonzero.

## V. SUMMARY AND DISCUSSION

We have described and applied a simple approach for calculating the effective conductivity (or dielectric constant), and the electric-field distribution, in a periodic composite. The method is applicable to both two- and three-dimensional systems, and is accurate for arbitrary concentrations of inclusions, conductivity contrasts, inclusion shapes, and numbers of components. It can readily be extended to anisotropic composite media, such as would be produced by placing an

isotropic metallic composite in an external magnetic field.

It is useful to compare the advantages and disadvantages of the method just described to others in the literature. The methods of Milton *et al.*, and of Bergman and collaborators, can be made extremely accurate, but in general they involve calculating a different set of basis functions for each geom-

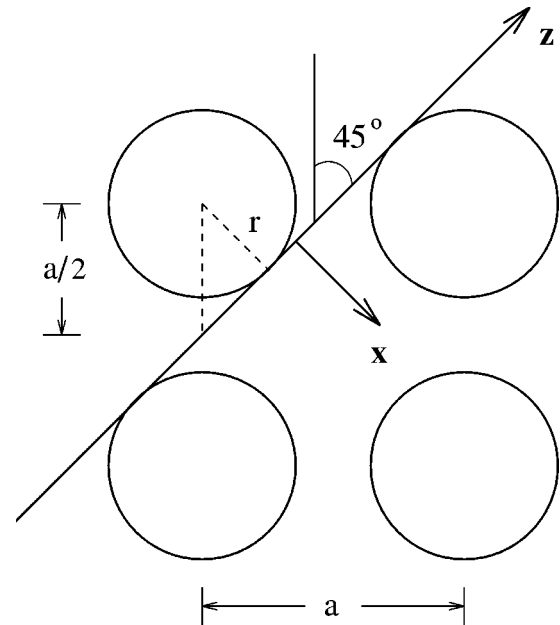


FIG. 6. Illustration of the percolation argument which determines  $p_c^*(\theta)$ , for the special case of circular inclusions and  $\theta = 45^\circ$ . A straight line is drawn at an angle  $\theta$  to the axis of the square lattice (lattice constant =  $a$ ).  $p_c^*(\theta)$  is determined as that areal fraction of inclusions ( $p = \pi r^2/a^2$ ) greater than which any such line is certain to intersect one or more  $S$  inclusions. From the triangle construction, we find  $p_c^*(45^\circ) = \pi/8 = 0.39$ .

etry. The methods using  $k$ -space expansions do not require such recalculation, but they may require large numbers of plane waves, since the composite dielectric functions change abruptly in real space. By contrast, the present method can be equally well applied to any geometry and filling fraction, and the inclusions need not have a convenient symmetrical shape, as is useful in the basis function approaches. On the other hand, the iterative relaxation scheme for solving these equations can converge quite slowly, and this may lead to inaccuracies. Other procedures, such as over- or under-relaxation, might provide more accuracy, or at least faster convergence to a solution, but we have not tested this possibility in the present paper. Finally, our approach is straightforward and direct to apply, requiring only the use of standard numerical methods for solving sets of linear inhomogeneous algebraic equations. Thus, in sum, each of the methods described here might be particularly convenient for different periodic composites.

Our numerical results for isotropic composites in two dimensions show that this approach is potentially as accurate as various existing analytical approximations for treating periodic composites. When we apply the method to periodic arrays of perfect conductors embedded in a normal-metal host, we find a striking anisotropy in the magnetoresistivity as a function of the applied magnetic field orientation within the plane of the array. The calculated anisotropy is consistent

with a simple percolation argument applied to anisotropic composites. Although no experiments seem to have been carried out for this geometry, a similar experiment, carried out for a periodic mesoscopic antidot array, yields a similar (and very large) anisotropy which is correctly reproduced by a semiclassical calculation such as ours.<sup>22</sup> Since fields such that  $\omega_c \tau = 10 - 50$  are readily attainable in many normal metals and lie below  $H_{c2}$  in many superconductors, it seems feasible that periodic NS arrays could be fabricated in which such experiments might be carried out.

Finally, we note that the approach used here can, in principle, be made arbitrarily accurate, subject only to the limitations of a finite mesh density and the convergence of the iterative algorithm. (Of course, it also depends on the assumption that the conductivity can be described without considering quantum corrections.) It should also work for complex conductivities, as expected at finite frequencies. Thus, the present simple approach may be useful for treating a variety of “classical” transport problems in periodic composites.

#### ACKNOWLEDGMENT

We gratefully acknowledge support from the NSF through NSF Grant No. DMR94-02131.

- 
- <sup>1</sup>G. W. Milton, R. C. McPhedran, and D. R. McKenzie, *Appl. Phys.* **25**, 23 (1981).
- <sup>2</sup>R. Tao, Z. Chen, and P. Sheng, *Phys. Rev. B* **41**, 2417 (1990).
- <sup>3</sup>L. C. Shen, C. Liu, J. Korringa, and K. J. Dunn, *J. Appl. Phys.* **67**, 7071 (1990).
- <sup>4</sup>D. J. Bergman and K. J. Dunn, *Phys. Rev. B* **45**, 13 262 (1992).
- <sup>5</sup>Lu Hui and Bao Ke-da, *Phys. Rev. B* **46**, 9209 (1992).
- <sup>6</sup>S. Datta, C. T. Chan, K. M. Ho, and C. M. Soukoulis, *Phys. Rev. B* **48**, 14 936 (1993).
- <sup>7</sup>D. J. Bergman and Y. M. Strelniker, *Phys. Rev. B* **49**, 16 256 (1994); **51**, 13 845 (1995); **50**, 14 001 (1994); **53**, 11 051 (1996).
- <sup>8</sup>B. Sareni, L. Krähenbühl, A. Beroual, and C. Brosseau, *J. Appl. Phys.* **80**, 1688 (1995).
- <sup>9</sup>For a recent review of the classical electromagnetic properties of composite media, including periodic composites, see, e.g., D. J. Bergman and D. Stroud, in *Solid State Physics: Advances in Research and Applications*, edited by H. Ehrenreich and D. Turnbull (Academic, New York, 1992), Vol. 46, pp. 177–269.
- <sup>10</sup>Periodic dielectrics have been reviewed in the context of photonic band structures and photonic band gaps by P. M. Hui and N. F. Johnson, *Solid State Physics: Advances in Research and Applications*, edited by H. Ehrenreich and F. Spaepen (Academic, New York, 1995), Vol. 49, p. 151.
- <sup>11</sup>See, e.g., E. Yablonovitch, *J. Phys.: Condens. Matter* **5**, 2443 (1993).
- <sup>12</sup>D. J. Resnick *et al.*, *Phys. Rev. Lett.* **47**, 1542 (1981).
- <sup>13</sup>D. W. Abraham *et al.*, *Phys. Rev. B* **26**, 5268 (1981).
- <sup>14</sup>R. F. Voss and R. A. Webb, *Phys. Rev. B* **25**, 3446 (1982).
- <sup>15</sup>R. Fogelholm and G. Grimvall, *J. Phys. C* **16**, 1077 (1983).
- <sup>16</sup>S. Kirkpatrick, *Rev. Mod. Phys.* **45**, 574 (1973).
- <sup>17</sup>D. Stroud, *Phys. Rev. Lett.* **44**, 1708 (1980).
- <sup>18</sup>J. C. Maxwell-Garnett, *Philos. Trans. R. Soc. London, Ser. A* **203**, 285 (1904).
- <sup>19</sup>Precisely at percolation, the “prism” geometry is self-dual, i.e., it is unaltered on interchanging the two components. For such a geometry,  $\sigma_e = \sqrt{\sigma_1 \sigma_2}$  exactly. This result is correctly given by the method of Milton *et al.* (Ref. 1) but seemingly not by that of Bergman and Dunn (Ref. 4). In our own calculations,  $\sigma_e$  always lies above this value for the finite networks we have considered, but, as shown in Table I, it is slowly approaching the correct limit as the network becomes larger. Of course, we cannot verify that the limit is actually reached for a very large network. We have checked that our particular discretization algorithm does indeed correctly give a self-dual network for  $p=0.5$ . The reasons for this slow convergence at percolation are not clear. We remark, however, that precisely at percolation,  $\sigma_e$  is extremely sensitive to details of the geometry. As we have verified, the discretized network we use necessarily always has a connected path of the larger conductivity across the sample, and this may account for the fact that our calculated  $\sigma_e$  is larger than the exact value at  $p_c$ .
- <sup>20</sup>See e.g., J. P. Straley, *J. Phys. C* **9**, 783 (1976).
- <sup>21</sup>H. J. Herrmann, B. Derrida, and J. Vannimenus, *Phys. Rev. B* **30**, 4080 (1984); D. J. Frank and C. J. Lobb, *ibid.* **37**, 302 (1988); C. J. Lobb and D. J. Frank, *ibid.* **30**, 4090 (1984); J. G. Zabolitzky, *ibid.* **30**, 4077 (1984).
- <sup>22</sup>M. Tornow, D. Weiss, K. v. Klitzing, K. Eberl, David J. Bergman, and Yakov M. Strelniker, *Phys. Rev. Lett.* **77**, 147 (1996).